

Electrochemical Mechanical Polishing of Flexible Stainless Steel Substrate for Thin-Film Solar Cells

Shuo-Jen Lee¹, Yi-Ho Chen^{1,*}, Chung Ping Liu², Tien Jung Fan³

¹Department of Mechanical Engineering, Yuan Ze University,

²Department of Photonics Engineering, Yuan Ze University,

³Department of Electrical Engineering, Yuan Ze University, Chung-Li, Taiwan, R.O.C.

*E-mail: yihoyzu@gmail.com

Received: 19 March 2013 / Accepted: 12 April 2013 / Published: 1 May 2013

The morphology of stainless steel is a key factor that affects the quality and structure of deposited cell material and, thus, the efficiency of flexible solar cells. Electrochemical mechanical polishing (ECMP) combines electrochemical and mechanical actions to reduce surface roughness to the level of tens of nano-meters for some metals. In this study, a novel ECMP system is introduced and electrochemical process parameters are evaluated. Finally, both stainless steel (SS) 304 and SS430 substrates sized 10 cm × 10 cm are polished from average roughness (R_a) of 35 nm, and peak roughness (R_p) of 126 nm down to an R_a of 10 nm and R_p of 65 nm. These roughness values are very close to that of glass substrates. Amorphous silicon solar cells are fabricated simultaneously on SS304-Bright Annealing (BA), SS304-ECMP, SS430-BA, and SS430-ECMP substrates in the same run. The substrates treated with ECMP have better cell performance than untreated substrates. This ECMP process is an efficient and economical method for producing a super smooth SS surface as the substrate for thin-film solar cells.

Keywords: Thin-film solar cell; stainless steel substrate; electrochemical mechanical polishing; surface morphology

1. INTRODUCTION

Thin-film solar cells such as Dye Sensitized Solar Cell (DSSC), Copper Indium Gallium Selenide (CIGS), and amorphous silicon, are hot topics in recent academic research and industry. To make solar cells flexible, stainless steel (SS) is one substrate material under consideration. Flexible solar cells fabricated on SS substrate are widely used for Building Integrated PhotoVoltaics (BIPVs). Stainless steel has many advantages, such as low cost, high strength, and ease of preparation. Chau *et*

al. argued that BIPVs, especially as rooftop panels, would form the largest market for flexible PV products [1]. Fung and Yang studied the impacts of different parameters of BIPV modules on the cell efficiency [2]. However, the main challenge is how to improve the cost-performance ratio of BIPVs [3]. Thus, their conversion efficiency is the key benchmark index. Python *et al.* proposed the relation between substrate surface morphology and microcrystalline silicon solar cell performance [4]. Chung demonstrated that the surface quality of the SS substrate of an amorphous silicon solar cell markedly influences on its service performance and lifespan [5]. Li *et al.* reported that structural defects caused by substrate roughness may cause a poor conversion efficiency for a thin film silicon solar cell [6]. Thus, SS substrate smoothness is desirable for flexible thin-film silicon solar cells.

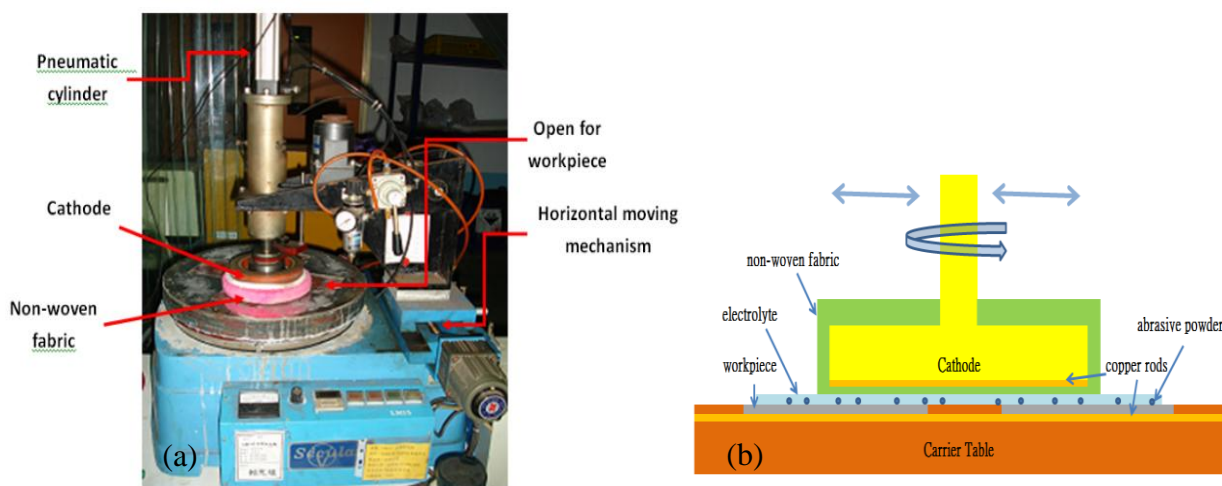


Figure 1. (a) An ECMP prototype system and (b) Schematic of electrodes, electrolyte and abrasive powders.

Electrochemical Mechanical Polishing (ECMP) is a compound polishing technique that combines the mechanical action of a grinding process with an electrochemical reaction of an Electrochemical Machining (ECM)-like process. Chen *et al.* characterized the basic reaction mechanism of ECMP [7]. Lee *et al.* identified the suitable process parameters for ECMP [8]. Figure 1(a) shows an ECMP prototype system. The workpiece is the anode, and the polishing pad is the cathode. When the gap between electrodes is filled with an electrolyte, a mixture of 10% sodium nitrate solution and alumina, Al_2O_3 , powders, the electrochemical reaction occurs under the applied voltage. Because the electrochemical reaction changes surface properties, a surface can be polished with increased efficiency by combining an electrochemical and mechanical planarization mechanism. When the electrochemical reaction starts, the reactant in the ECMP process is generally a metallic hydroxide, $\text{M}(\text{OH})_n$, and/or metallic oxide, MO_x , which are removed in the subsequent mechanical polishing process. This metallic hydroxide or oxide is of thickness of about a few nm to several μm thick and is easily polished away by an abrasive medium, such as Al_2O_3 [7].

The electrochemical polishing mechanisms of ECMP are examined with the linear polarization method for both SS304 and SS430. The linear polarization method has been employed widely to

characterize the electrochemical properties of a material after surface treatment [9]. The I-V curve of an electrochemical reaction provides material information such as reaction trend, active voltage, and exchange current density. Therefore, the I-V curves are employed in this study to evaluate the effects of the electrolyte concentration and help identify the suitable electrochemical parameters for ECMP.

2. SYSTEM SET-UP

The ECMP system (Figure 1(a)) has three major components: electrodes, rotational mechanism, and power supply. Figure 1(b) shows the relationships between electrodes, abrasives, and electrolyte.

The Cathode (polishing pad): The cathode is made of copper rods embedded in a Bakelite disk. These copper rods conduct the electrical current to the electrolyte in the gap between electrodes. Additionally, the Bakelite disk is covered by a non-woven fabric to ensure that abrasive powders adhere to it when the cathode is rotating and that the mechanical polishing mechanism will function properly. The cathode rotational speed is around 50 rpm.

The Anode (carrier table): Similar to the cathode, the anodic carrier table is a Bakelite disk with embedded copper rods. The top surface of the table is covered by an SS plate as a fixture with some desired openings for placing workpieces. This system has five openings, each sized 10 cm × 10 cm. Table rotational speed is approximately 90 rpm.

The horizontal moving mechanism of the cathode: To improve process uniformity, the cathode is fixed on a screw rod moving horizontally. The distance that the screw rod moves is 30 cm and the moving speed of the screw rod is 0.1–1.4 mm/sec.

The pneumatic cylinder for cathode press pressure: To control and adjust the press force of the cathode on the carrier table, a pneumatic cylinder is fixed on the cathode top. The cylinder is connected to a compressed air source and air pressure is adjustable using a valve.

3. ECMP PROCESSING PARAMETERS

3.1. The electrolyte

Salts, such as NaNO₃, NaCl and Na₂SO₄, are generally used as the electrolyte for ECMP. In this study, NaNO₃ is chosen because of its good electrochemical and chemical properties such as neutral pH, minimal corrosiveness, and less intergranular corrosion (IGC) attack [10]. Three electrolytes are tested. Electrolyte A is 10% NaNO₃ solution; electrolyte B is 10%wt NaNO₃ solution and 5%wt glycerin; Electrolyte C is 10%wt NaNO₃ solution and 10%wt glycerin. The glycerin in the electrolyte improves the surface quality [11]. The I-V curves of three electrolytes, no additive, 5% glycerin, and 10% glycerin, for each of the two materials, SS430 and SS304 are measured (Figure 2 (a) and (b)). Finally, the electrolyte with 10% glycerin is chosen because its I-V curve has the lowest current density at the plateau region.

3.2. Abrasive powder

Table 1. The roughness comparison of using three abrasives for polishing 50 minutes.

| Abrasive type | Cathode rpm | Anode rpm | R _a (μm) | R _p (μm) |
|---|-------------|-----------|---------------------|---------------------|
| SiC (1-μm) | 45 | 25 | 0.026 | 0.211 |
| Al ₂ O ₃ (1-μm) | 45 | 25 | 0.010 | 0.096 |
| Al ₂ O ₃ (0.5-μm) | 45 | 25 | 0.010 | 0.086 |

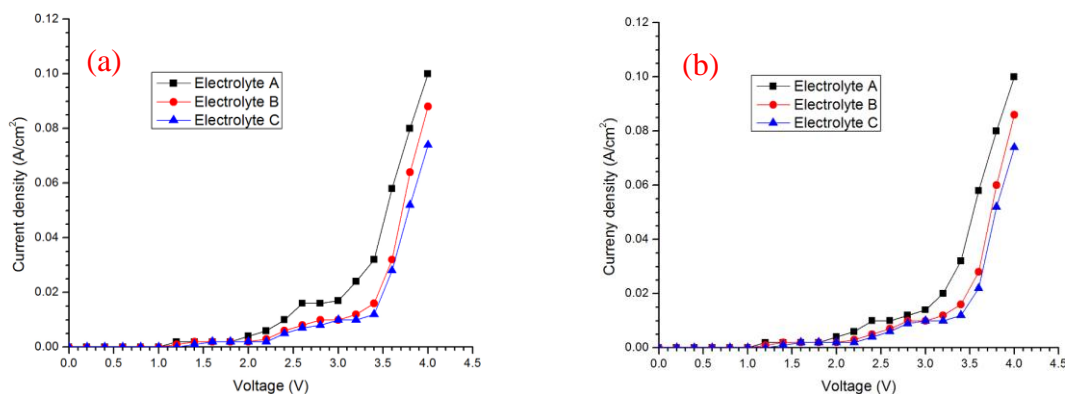


Figure 2. I-V curves with different electrolytes for (a) SS430 and (b) SS304.

Alumina (Al₂O₃), silicon carbide (SiC), and silicon oxide (SiO₂) are the most popular abrasive powders applied in the CMP process [12,13]. Alumina powders with a diameter of 1 μm and 0.5 μm are added separately to the electrolyte at the volume ratio of 10%. Table 1 lists the surface roughness values when using the two diameters of Al₂O₃ powder after 50 minutes of ECMP. The 0.5-μm Al₂O₃ powder produces better surface roughness than the 1-μm powder.

3.3. Voltage and current density

Although the net current density of the electrochemical reaction in the ECMP process is a critical parameter, it is difficult to calculate because the electrical current passes many components and materials (e.g., copper, carbon, SS and electrolyte). During the ECMP process, the reaction area is always changing due to rotation of the workpiece and cathode. The easiest way to adjust current density is to change applied voltage, which is controlled by the power supply. Electrical voltages of 3 V and 7 V are applied to the ECMP system for comparison. Table 2 lists comparison results. At 3 V, the current value on the power supply is about 0.01–0.04 A/cm², and at 7 V, the value is about 0.05–0.12 A/cm². The surface of the SS430 workpiece look dull at 7 V, regardless of which electrolyte is used (Figure 3(a)). Figure 3(b) and 3(c) show the shiny appearance of SS430 and SS304 at the low applied voltage of 3 V.

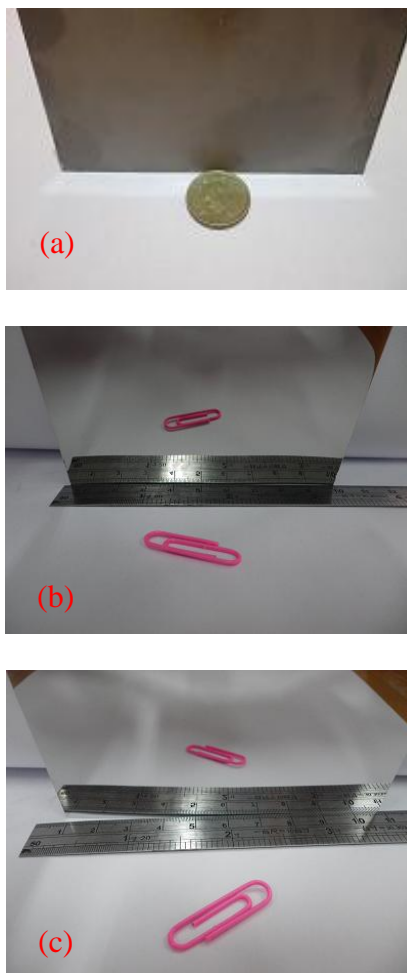


Figure 3. The surface appearance of workpieces after ECMP: (a) SS430 at 7 V;(b) SS430 at 3 V;(c) SS304 at 3 V.

Table 2 lists the surface parameters after ECMP under different electrolytes and applied voltages. The low current density eliminates surface dullness after an ECMP treatment. The electrolyte with 10% glycerin produces better surface gloss than the electrolyte with 5% glycerin. The dull surface of SS430 is analyzed by Scanning Electron Microscope (SEM). The SEM results show that there is more than 4% (atomic ratio) of carbon on the surface of the dull SS430. The SS430 is a Ferrite with a body cubic crystal (BCC) structure. Only a small amount of carbon could be dissolved in Ferrite. The dissolved carbons are easy to form dislocations in the material structure of SS430. When high voltage is applied, the electrochemical reaction is strong. The surface of SS430 dissolved rapidly, but carbon could not be dissolved as fast into the electrolyte or moved away from the surface. This likely explains why the SS430 surface becomes dull after ECMP at high voltage. Thus, applied voltage is fixed at 3 V for future experiments to ensure that the workpiece can be polished properly.

Table 2. The surface parameters of ECMP with three different electrolytes. (Rotational speed: Cathode 45 rpm, Anode 25 rpm.)

| | Electrolyte additive | Voltage (V) | Polishing Time (minute) | R _a (μm) | R _p (μm) | Surface appearance |
|-------|----------------------|-------------|-------------------------|---------------------|---------------------|--------------------|
| Set 1 | NA | 7 | 10 | 0.32 | 1.12 | dull |
| Set 2 | NA | 3 | 10 | 0.12 | 0.88 | little shining |
| Set 3 | Glycerin 5% | 7 | 10 | 0.28 | 1.04 | dull |
| Set 4 | Glycerin 5% | 3 | 10 | 0.11 | 0.68 | little shining |
| Set 5 | Glycerin 10% | 7 | 10 | 0.3 | 1.1 | dull |
| Set 6 | Glycerin 10% | 3 | 10 | 0.12 | 0.74 | shining |

3.4. Press force and rotational speeds of the cathode and anode

The press force from the cathode to the anode and the rotational speeds of the cathode and anode have both electrochemical and mechanical polishing effects. From a mechanical polishing point of view, high press force and high rotational speed increase abrasive efficiency. However, from an electrochemical polishing point of view, getting the electrolyte into the gap between the electrodes when press force is high is difficult. Therefore, a balance that ensures that both mechanical and electrochemical mechanisms function well is needed. Due to a limitation of the prototype ECMP system, maximum press pressure is around 5 kg/cm². The carrier table stalls when the press pressure exceeds 1.2 kg/cm². Thus, 1.0 kg/cm² press pressure is chosen for the following experiments. To identify the optimal rotational speeds for the cathode and anode, three rotational speeds are tested (Table 3). The test with the cathode rotating at 45 rpm and the anode rotating at 25 rpm yields the best roughness values of R_a of 0.01 μm and R_p of 0.09 μm.

Table 3. The roughness comparison with various rotational speeds of the cathode and the anode, Abrasive type: Al₂O₃ (0.5 μm).

| | Cathode (rpm) | Anode (rpm) | Electrolyte | R _a (μm) | R _p (μm) |
|--------|---------------|-------------|-----------------------|---------------------|---------------------|
| Test 1 | 45 | 25 | 15% NaNO ₃ | 0.010 | 0.090 |
| Test 2 | 25 | 25 | 15% NaNO ₃ | 0.015 | 0.102 |
| Test 3 | 45 | 45 | 15% NaNO ₃ | 0.010 | 0.098 |

3.5. Polishing time

To identify the optimal polishing time, surface roughness value must be measured at different times. Both the SS304-Bright Annealing (BA) and SS430-BA plates are 100 μm thick and sized 10 cm × 10 cm for ECMP testing. Figures 4(a) and 4(b) show the changes in R_a and R_p values over time. When voltage is applied, the workpiece has the lowest R_p of 0.065 μm at around 10 minutes. More

than 20 minutes is needed to reach the lowest R_p of $0.086 \mu\text{m}$ with zero voltage. The $0.5\text{-}\mu\text{m}$ abrasive powder has better performance than $1\text{-}\mu\text{m}$ abrasive powder. Applied voltage of 3 V generates the best surface quality.

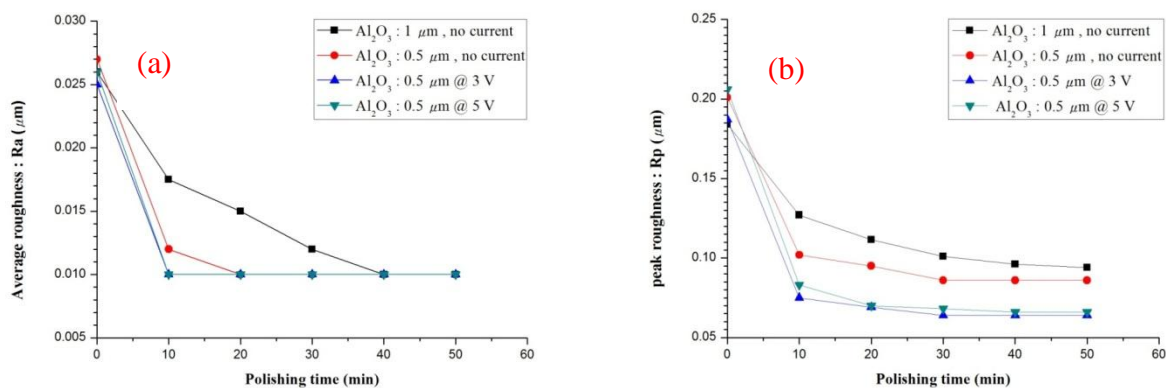


Figure 4. The roughness values under different process parameters: (a) Average Roughness (R_a); (b) Peak Roughness (R_p).

At 3 V applied voltage, the R_a value decreases to $0.01 \mu\text{m}$ at only 10 minutes but 20 minutes is required to reach an R_a of $0.01 \mu\text{m}$ when no voltage is applied. This indicates that the electrochemical mechanism may have contributed 50% to total efficiency of the ECMP. Both SS304 and SS430 have mirror-like surface quality after 10 minutes. Therefore, the most efficient polishing time is around 15 minutes.

4. FABRICATION OF AMORPHOUS SILICON THIN-FILM SOLAR CELLS

The amorphous silicon thin-film solar cells were fabricated on SS304-BA, SS304-ECMP, SS430-BA, and SS430-ECMP substrates in the same run. Table 4 lists the surface roughness of these four SS substrates. These four substrates were processed simultaneously in the same chamber by high-frequency plasma-enhanced chemical vapor deposition (HF-PECVD) in an ultra-high-vacuum, single-chamber, load-locked system at a constant temperature of 200°C . The cell structure was SS/Ag/AZO/n-i-p/AZO/Ag. The 60-nm -thick Ag layer was deposited as a back reflector layer and back contact on the substrate by radio frequency (RF) magnetron sputtering. The alumina-zinc-oxide (AZO) buffer layer, which had a thickness of 30 nm , is essential in improving the interface between the metal and semiconductor material. For silicon layer deposition, the a-SiC:H was prepared by high-frequency PECVD using pre-determined parameter values. Table 5 presents deposition parameters of the intrinsic and doped silicon films. The AZO film was coated on the SS substrate by radio frequency magnetron sputtering with base pressure of 5×10^{-7} torr and power of 800 W at room temperature. The front Ag electrodes were deposited by sputtering at 20 W at room temperature. Finally, a solar simulator was utilized to characterize these cells with current-voltage measurements under 100 mW/cm^2 and Air Mass (AM) 1.5.

Table 4. The surface roughness of SS304 and SS430 substrates

| Material | R _a (μm) | R _p (μm) |
|------------|---------------------|---------------------|
| SS304 ECMP | 0.01 | 0.0642 |
| SS430 ECMP | 0.01 | 0.0624 |
| SS304 BA | 0.027 | 0.20 |
| SS430 BA | 0.026 | 0.19 |

Table 5. The PECVD parameters of deposition of intrinsic and doped silicon

| | p | b | i | n |
|--------------------------------------|-----|-----|-----|-----|
| Pressure(Pa) | 90 | 90 | 90 | 60 |
| Power(W) | 10 | 10 | 10 | 10 |
| E/S(mm) | 20 | 20 | 30 | 25 |
| Temp(°C) | 200 | 200 | 200 | 200 |
| Thickness (nm) | 8 | 6 | 250 | 30 |
| SiH ₄ (sccm) | 20 | 20 | 40 | 40 |
| H ₂ (sccm) | 160 | 160 | 160 | 80 |
| PH ₃ (sccm) | -- | -- | -- | 5 |
| B ₂ H ₆ (sccm) | 5 | -- | -- | -- |
| CH ₄ (sccm) | 15 | 15 | -- | -- |
| Pressure(Pa) | 90 | 90 | 90 | 60 |
| Power(W) | 10 | 10 | 10 | 10 |

5. DISCUSSION

In previous ECMP experiments, the optimized parameters were 3 V, 0.5-μm abrasive powder, and electrolyte with 10% glycerin. Figures 5(a)–(d) show pictures of the surface morphology of specimens before and after ECMP measured by an optical microscope. The optical properties of the four substrates were measured by a UV-visible-near-IR spectrophotometer (Perkin Elmer Lambda 750s) in the 300–700 nm wavelength range (Figure 6(a) and 6(b)). Average total reflection (TR) rate increased from 68.1% for the untreated 430 SS substrate to 69.3% for the ECMP-processed 430 SS substrate, and from 62.1% for the untreated 304 SS substrate to 67.5% for the ECMP-processed 304 SS substrate. Average diffuse reflection (DR) rate decreased from 4.1% for the untreated 430 SS substrate to 1.1% for the ECMP-processed 430 SS substrate, and from 6.3% for the untreated 304 SS substrate to 1.1% for the ECMP-processed 304 SS substrate. Table 6 lists cell performance of different substrates, and Figure 7 lists their J-V characteristics. All the cells' processes on the untreated and ECMP-processed SS304 and SS430 were finished in the same run. Thus, the major difference is surface morphology.

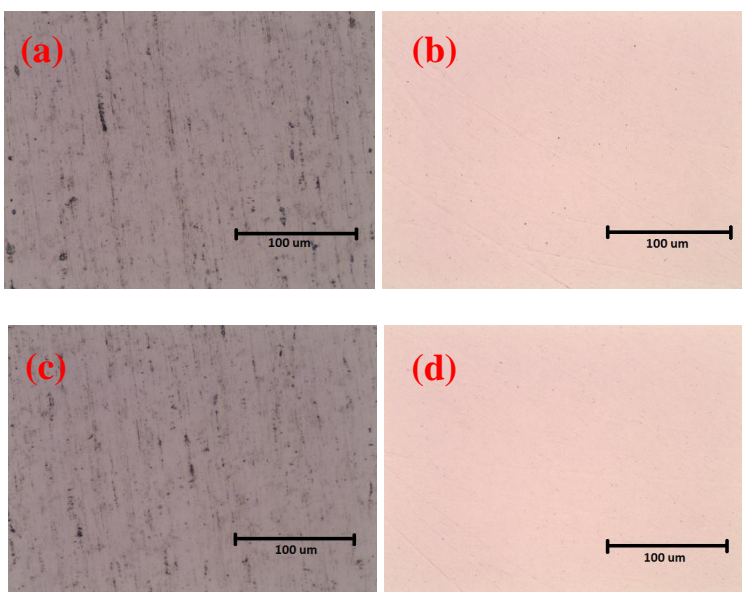


Figure 5. The surface morphology measured by OM: (a) SS304 BA; (b) SS304 after 20 minutes ECMP; (c) SS430 BA; (d) SS430 after 20 minutes ECMP.

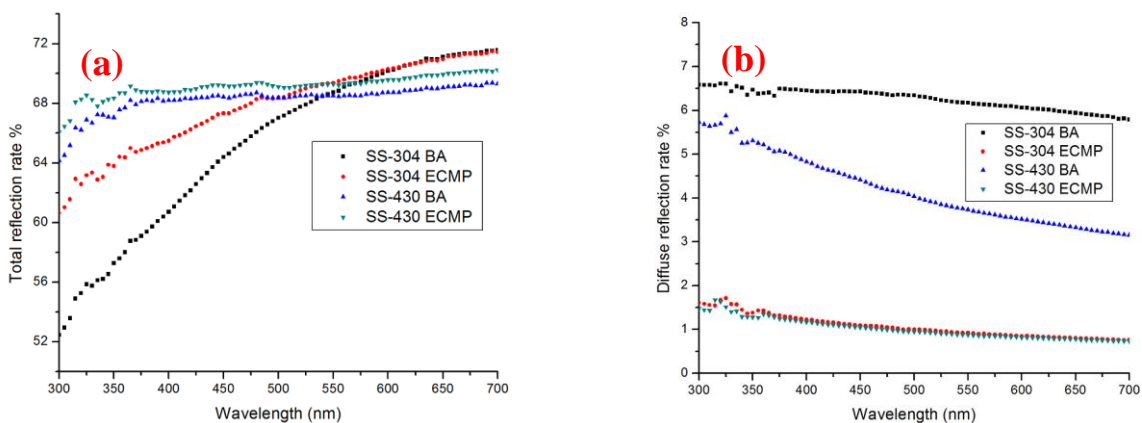


Figure 6. The optical properties of SS substrates: (a) the total reflection (TR) rate; (b) the diffuse reflection (DR) rate.

A rough substrate may result in micro-cracks during deposition of the silicon layer and cause poor conversion efficiency of thin-film silicon solar cells [6]. From our experiment, the conversion efficiency of a-Si:H thin-film solar on untreated 430SS and 304SS substrate was 3.6% and 3.3%, and could be improved to 5.4% and 5.1% on 430SS and 304SS ECMP-processed substrates accordingly. Both SS304 and SS430 substrates treated by ECMP have better efficiency than the substrates not treated by ECMP. As the thermal expansion coefficient of 430 SS is closer to silicon than SS304, SS430 seems a better choice than SS304 as the substrate of a thin-film solar cell.

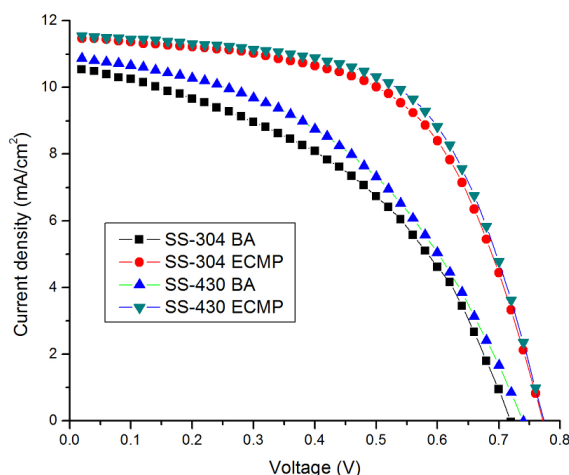


Figure 7. The J-V curves of SS-304BA, SS-304ECMP, SS430-BA and 430-ECMP substrates.

Table 6. The performance comparison of thin film solar cells on different substrates (cell size: 10 x 10 mm)

| | V_{oc} (V) | J_{sc} (mA/cm ²) | FF (%) | η (%) |
|--------------|-----------------|-----------------------------------|-----------|---------------|
| SS 304-BA | 0.71 | 10.6 | 44 | 3.3 |
| SS 304- ECMP | 0.77 | 11.4 | 58 | 5.1 |
| SS 430-BA | 0.73 | 10.9 | 45 | 3.6 |
| SS 430-ECMP | 0.77 | 11.5 | 60 | 5.4 |

6. CONCLUSIONS

The following conclusions are based on experimental results.

1. Abrasive powders with a small diameter produce lower surface roughness of the workpiece in ECMP than powders with a large diameter.
2. With an electrochemical reaction, polishing efficiency can be improved to around 50%, and the final roughness values of R_a and R_p are reduced.
3. Polishing time of 15–20 minutes is appropriate for ECMP. A longer polishing time cannot reduce the roughness further.
4. The addition of glycerin to the electrolyte reduces the electrical conductivity of the electrolyte, and the current density of the electrochemical reaction is reduced.
5. High applied voltage and high current density accelerate the electrochemical reaction more than the mechanical abrasive process. Therefore, the workpiece surface looks dull when the applied voltage is high.
6. The surface roughness of SS304 and SS430 of around R_a of 0.027 μm and R_p of 0.22 μm before ECMP were improved to R_a of 0.01 μm and R_p of 0.062 μm within 20 minutes.
7. The ECMP treatment improves the surface flatness of SS substrate, resulting in enhanced solar cell performance.

ACKNOWLEDGEMENTS

The authors gratefully acknowledge the financial support from Chung-Shang Institute of Science and Technology, Taiwan, R.O.C. under contract no. CSIST-769-V201.

References

1. J.L.H. Chau, R.-T. Chen, G.-L. Hwang, P.-Y. Tsai, C.-C. Lin, *Sol. Energy Mater. Sol. Cells*, 94 (2010), 588-591.
2. T.Y.Y. Fung, H. Yang, *Energy & Buildings*, 40 (2008), 341-350.
3. S.-J. Lee, C.-Y. Lin, S.-L. Cheng, W.-C. Ke, *Mater. Chem. and Phys.* 130 (2011), 733-737.
4. M. Python, E. Vallat-Sauvain, J. Bailat, D. Domine, L. Fesquet, A. Shah, C. Ballif, *J. Non-Crystalline Solids*, 354 (2008), 2258-2262.
5. Y.-C. Chung, *The effect of surface morphology on silicon thin film solar cell with stainless steel substrate*. Master thesis (2011), Yuan Ze University, Taiwan.
6. H.B.T. Li, R.H. Franken, J.K. Rath, R.E.I. Schropp, *Sol. Energy Mater. and Sol. Cells*, 93 (2009), 338-349.
7. Y.-L. Chen, S.-M. Zhu, S.-J. Lee, J.-C. Wang, *J. Mater. Processing Tech.*, 140 (2003), 203-205.
8. S.-J. Lee, Y.-M. Lee, M.-F. Du, *J. Mater. Processing Tech.*, 140 (2003), 280-286.
9. J. Kupis, H. Scholl, O. Vittori, *Electrochimica Acta*, 37 (1992) 2523-2532.
10. J. Y. Wang, J.W. Xu, *The principles and applications of electrochemical machining*, National Defense Industry Press (2011), Beijing.
11. C.-C. Lin, C.-C. Hu, T.-C. Lee, *Surf. and Coat. Tech.* 204 (2009), 448-454.
12. H. Lei, L. Jiang, R. Chen, *Powder Tech.*, 219 (2012), 99-104.
13. G.-S. Pan, Z.-H. Gu, Y. Zhou, T. Li, H. Gong, Y. Liu, *Wear*, 273 (2011), 100-104.